

to appear in ApJS

The VSOP 5 GHz AGN Survey II. Data Calibration and Imaging

J. E. J. Lovell ¹, G. A. Moellenbrock ², S. Horiuchi ³, E. B. Fomalont ⁴, W. K. Scott ⁵,
H. Hirabayashi ⁶, R. G. Dodson ⁶, S. M. Dougherty ⁷, P. G. Edwards ⁶, S. Frey ⁸,
L. I. Gurvits ⁹, M. L. Lister ¹⁰, D. W. Murphy ¹¹, Z. Paragi ⁹, B. G. Piner ¹², Z.-Q. Shen ¹³,
A. R. Taylor ⁵, S. J. Tingay ³, Y. Asaki ⁶, D. Moffett ¹⁴, Y. Murata ⁶

ABSTRACT

The VSOP mission is a Japanese-led project to study radio sources with sub-milliarcsecond angular resolution using an orbiting 8-m telescope, HALCA and global arrays of Earth-based telescopes. Approximately 25% of the observing

¹Australia Telescope National Facility, Commonwealth Scientific and Industrial Research Organization, P. O. Box 76, Epping NSW 2122, Australia

²National Radio Astronomy Observatory, P.O. Box 0, Socorro, NM 87801, USA

³Centre for Astrophysics and Supercomputing, Swinburne University of Technology, P.O. Box 218, Hawthorn, Victoria 3122, Australia

⁴National Radio Astronomy Observatory, 520 Edgemont Road, Charlottesville, VA 22903, USA

⁵Physics and Astronomy Department, University of Calgary, 2500 University Dr. NW, Calgary, Alberta, Canada, T2N 1N4

⁶Institute of Space and Astronautical Science, Japan Aerospace Exploration Agency, 3-1-1 Yoshinodai, Sagami-hara, Kanagawa 229-8510, Japan

⁷Dominion Radio Astrophysical Observatory, P.O. Box 248, White Lake Road, Penticton, BC, Canada V2A 6K3

⁸FÖMI Satellite Geodetic Observatory, P.O. Box 585, H-1592, Budapest, Hungary

⁹Joint Institute for VLBI in Europe, P.O. Box 2, 7990 AA, Dwingeloo, The Netherlands

¹⁰Physics Department, Purdue University, 525 Northwestern Ave, W. Lafayette IN, 47907-2036

¹¹Jet Propulsion Laboratory, 4800 Oak Grove Drive, Pasadena, CA 91109, USA

¹²Department of Physics & Astronomy, Whittier College, 13406 E. Philadelphia St., Whittier CA 90608, USA

¹³Shanghai Astronomical Observatory, 80 Nandan Rd., Shanghai 200030, P.R.China

¹⁴Physics Department, Furman University, 3300 Poinsett Highway, Greenville, SC 29613, USA

time has been devoted to a survey of compact AGN at 5 GHz which are stronger than 1 Jy — the VSOP AGN Survey. This paper, the second in a series, describes the data calibration, source detection, self-calibration, imaging and modeling, and gives examples illustrating the problems specific to space VLBI. The VSOP Survey web-site which contains all results and calibrated data is described.

Subject headings: galaxies: active — radio continuum: galaxies — surveys — techniques: interferometric

1. Introduction

On 1997 February 12, the Institute of Space and Astronautical Science (ISAS) launched the HALCA satellite carrying an 8m radio telescope dedicated specifically to Very Long Baseline Interferometry (VLBI). With an apogee height of 21400 km, radio sources are able to be imaged with angular resolution three times greater than with Earth-based arrays at the same frequency (Hirabayashi et al. 1998). About 25% of the observing time to date has been dedicated to the VSOP AGN Survey of ≈ 400 flat-spectrum AGN which are stronger than 1 Jy at 5 GHz. Observations from the VLBA Pre-Launch Survey (hereafter VLBApl, Fomalont et al. 2000b) revealed that 294 of these sources demonstrated compact structures suitable for observations with HALCA, and these were included in the VSOP Source Sample (VSS). (This number was initially reported as 289 [Hirabayashi et al. (2000b)] but increased to 294 when it was found that the use of low accuracy positions had initially resulted in 5 other sources not being detected [Edwards et al. (2002)].) The compilation and general description of the VSOP AGN Survey is given by Hirabayashi et al. (2000b) (Paper I) and Fomalont et al. (2000a). The major goal of the Survey is to determine statistical properties of the sub-milliarcsecond structure of the brightest extragalactic radio sources at 5 GHz, and to compare these structures with other properties of the sources. Combined with ground observations at many radio frequencies (single-dish and VLBI) and at higher energies, the Survey will provide an invaluable source list for detailed ground-based studies, as well as list of sources for future space VLBI missions.

In this paper, the second in the VSOP Survey series, we describe the data calibration and imaging procedures adopted for the VSOP Survey Program. These procedures are sufficiently different from more conventional VLBI data reduction because of the relatively poor phase stability and low signal-to-noise inherent in space VLBI. Paper III (Scott et al. 2004) presents results for the first 102 sources and Paper IV (Horiuchi et al. 2004) contains a statistical analysis using the visibility data for sources with $\delta > -44^\circ$.

In §2 we briefly review the correlation of VSOP data. In §3 we discuss the calibration procedure, and in §4 we outline the self-calibration, imaging and modeling of the sources. Finally, in §5 we describe the VSOP web site and its access.

2. Correlation of VSOP Data

The VLBI Space Observatory Programme (VSOP) was described in detail by Hirabayashi et al. (2000a,b). For the Survey, the VLBI wavefront data are recorded in the standard HALCA continuum mode at each participating ground telescope, and HALCA data are similarly recorded by one or more of the five tracking stations (see Paper I). The delays in the downlink from the spacecraft to each tracking station were also monitored at the tracking stations (Hirabayashi et al. 2000a). Four recording formats have been used in VSOP observations: VLBA (Napier et al. 1994), MkIV (Whitney 1999), S2 (Carlson et al. 1999) and VSOP (Shibata et al. 1998). For many Survey observations, a mixture of recording formats are used at the tracking stations and ground telescopes; in these cases, special-purpose devices located at the VSOP correlator in Mitaka, Japan are used to translate the data to a common format, which is then supplied to the appropriate correlator. The majority of the Survey experiments were correlated with the S2 Correlator (DRAO, Penticton, BC, Canada) until 2002 August. The VSOP correlator (NAOJ, Mitaka, Japan) has been used for some of the observations which included the ground telescopes at Usuda and Kashima, and has been used for all observations after 2002 August. The VLBA correlator (NRAO, Socorro, NM, USA) was used until early 2002 for many of the General Observing Time (GOT) experiments in VLBA and Mk4 formats, from which a sub-set of the data was extracted for use in the Survey (Hirabayashi et al. 2000b). Data are exported from each correlator in a format appropriate for initial reduction in the NRAO AIPS package (Greisen 1988).

The correlator output consists of typically 128 frequency channels in each of two 16 MHz bands. The VLBA and Penticton correlators produced data at time-samplings of 0.5 seconds and 2.0 seconds for space-ground and ground-only baselines respectively while the Mitaka correlator produces data at a 1 second sampling on all baselines. Thus the data have sufficient resolution to search for fringes within a window spanning a residual delay of $\pm 4\mu\text{sec}$ and a residual phase-rate of 1 Hz. This corresponds to a position error of 500 m and velocity error of 3 cm/s for the HALCA satellite, significantly larger than the nominal errors of the orbit determination (Hirabayashi et al. 2000a).

The translation integrity and the relative amplitude scaling of the three correlators were checked using the results of several three-hour experiments in which a strong source was observed using three ground stations, two of which could record data simultaneously

in two formats. The data were processed through all three correlators (with format translations made as necessary), and the results were compared. First, it was found that the translation process did not change the correlated amplitude by more than 2%, except when there were clear indications of recording problems. Second, the comparison of the visibility amplitudes for the same experiment processed by each correlator established the relative correlator amplitude scale factor to an accuracy of 3% (G. A. Moellenbrock et al. 2002, private communication).

3. Data Calibration and Detection

The reduction of VSOP Survey observations is being undertaken by a global effort of astronomers with an interest in high-resolution imaging. Therefore, a set of reduction procedures has been developed to ensure, as much as possible, that the Survey results are internally consistent.

The reduction procedure consists of two main parts. The first part, covered in this section, consists of initial calibration and fringe-fitting, and is performed using the NRAO AIPS package. The second part, covered in §4 consists of self-calibration, imaging and model-fitting, and is performed using the Caltech Difmap package (Shepherd 1997). The following sections describe these steps in detail with AIPS tasks and Difmap commands indicated by text in the SMALL CAPS style.

3.1. Preliminaries and *a priori* Calibrations.

The correlator distribution data for each experiment is imported into NRAO AIPS using the task FITLD. The datasets are sorted, indexed, and documented using standard AIPS tasks (MSORT, INDXR, LISTR, PRTAN, DTSUM). Except for datasets correlated in Penticton, it is necessary to run ACCOR to remove fringe normalization errors arising from potentially non-optimal sample populations among the four 2-bit voltage levels recorded at each telescope.

For *a priori* amplitude calibration, system temperature and gain information supplied by each telescope are imported into the AIPS database using ANTAB. Then, APCAL is used to form the $\sqrt{\text{SEFD}}$ calibration factors required to scale each antenna’s gain¹. For HALCA,

¹The *System Equivalent Flux Density (SEFD)* is the ratio of the system temperature (K) and telescope gain (K/Jy). It concisely describes the sensitivity of a radio telescope and the geometric mean of SEFD

the nominal 5 GHz system temperature is ~ 90 K and stable within an observation to $\sim 5\%$. Its SEFD was monitored early in the mission using total power observations of Cas A, Cyg A or Tau A and found to be relatively constant. The 5 GHz gain is 0.0062 K/Jy and this yields a HALCA SEFD of $\sim 14,500$ Jy, which is more than an order of magnitude larger than most ground telescopes. The *a priori* amplitude calibration value and reliability from the ground telescopes varies considerably, and can be in error by 30% for telescopes which are only occasionally used for VLBI.

As VSOP observations are made with global arrays of ground telescopes, it is not uncommon for some telescopes to be observing at frequencies in the 5 GHz band offset from their standard frequencies, i.e., the frequencies at which the nominal gain is measured and monitored. HALCA’s 5 GHz system noise temperature varies by almost 15% across the 4700–5000 MHz band (Kobayashi et al. 2000) and so Survey observations are generally scheduled at the frequencies where (the least sensitive telescope) HALCA’s performance was best. Use of nominal gain and nominal system temperature values, or even measured system temperature values if these were measured at the standard frequencies rather than the actual observing frequencies, also contributed to the overall uncertainties in gain calibration of VSOP Survey observations. Further amplitude corrections are discussed in the next sections, and Paper III describes a more accurate post-facto determination of the amplitude calibration of the Survey sources as a whole.

3.2. Fringe-fitting

Fringe-fitting, the process by which the correlated signals are detected, is the most important part of the Survey reductions. Unlike most ground-only VLBI, fringe detection for HALCA observations is difficult due to the limited sensitivity of the orbiting telescope, the generally lower correlated flux densities on long baselines and the larger uncertainty in the spacecraft’s location and clock. (The “spacecraft clock” is the hydrogen maser at the tracking station in use at the time, however the corrections required to correct for the downlink of the data introduced uncertainties in addition to those encountered for ground radio telescopes [Hirabayashi et al. 2000a].) This combination of conditions requires fringe searches for weak signals over large ranges of delay and fringe rate, hence the need for high time and frequency sampling. The small number of ground telescopes typical of Survey observations limits the sensitivity for global fringe-fitting as well (Cotton 1995). It is therefore important to limit

for two telescopes and provides the proper scaling factor to convert normalized correlation coefficients to Janskys.

the range of the search in delay and fringe rate as much as possible in order to keep the fringe searching efficient, and to avoid false detections. For many Survey datasets, delay and fringe rate solutions are available from fringe searches performed for data quality analysis at the correlators. Application of these delay and phase-rate offsets using CLCOR before more detailed fringe searching allows for significant data averaging and smaller fringe-search windows. For datasets with strong fringes for only a portion of the observation, the resulting narrower search should, in principle, allow detection of the weaker fringes. In practice, however, these gains have been modest.

For most observations, the AIPS task FRING is used for fringe-fitting. Solution intervals of up to 10 minutes (approaching the coherence time) are attempted to maximize the Signal-to-Noise Ratio (SNR). For strong sources, solution intervals as short as 2 minutes can be used as long as the SNR is greater than about 5. Detections are best gauged by consistency in the delay and fringe rate solutions between the two independent frequency channels (see Figure 1). For the weakest sources (few or no detections in the correlator’s data quality search), the AIPS task KRING was used since it allows larger searches and longer integrations than FRING for the same computer resources. Most of the editing of the data was obvious from the loss of detection during the fringing process, and from the telescope logs.

After an adequate fringe-fitting solution is obtained, the combined calibration was applied using SPLIT or SPLAT, which also averages the corrected data in frequency within each 16 MHz band, and to a common 2-second integration time. The data were then stored using FITTP or FITAB for subsequent processing.

4. Determining the Source Structure

In their analysis of VSOP observations of a complete sample of northern sources with very good (u, v) coverage on ground-only baselines, Lister et al. (2001) found that the dynamic range of a VSOP image is limited by poor sampling of the (u, v) plane on ground-space baselines. They found that the true dynamic range is between 30:1 and 100:1 depending on source complexity. In the case of VSOP Survey data this problem is amplified by the smaller number of ground radio telescopes and great care must be taken in interpreting the data. Although every effort was made to include long ground baselines in the scheduled array, this was not always achievable in practice. In general, VSOP Survey data provides a general idea of structure such as core sizes and intensities and basic jet properties such as position angle and location with respect to the core.

It is therefore important for the data analyst to keep these limitations in mind when

working with this sparsely sampled (u, v) -data with low SNR. Each stage of the data reduction must be checked in order to obtain a source structure which is consistent with the limitations in the data as well as incorporating *a priori* information about the source structures, either from the ground-only baselines or from other ground-based VLBI observations of the source. The Difmap software package was chosen for this part of the processing since it provides a good interface for viewing data, as well as visibility-plane model-fitting and image deconvolution facilities.

4.1. First-Pass Editing and Checking

The data from the AIPS calibration (2 s sampling in two single-channel frequency bands) are read into Difmap and averaged to a 30 s grid. The weights are calculated as the reciprocal of the data variance, which is proportional to the inverse square of the RMS. The data are then phase self-calibrated with a point source model on a 30 s timescale to determine the telescope-based phase as a function of time. Further data editing is based on several criteria: (1) Obvious outliers in a plot of amplitude versus projected (u, v) -distance are removed using RADPLOT; (2) Periods of low visibility amplitude for any antenna are found using VPLOT; (3) Periods of very poor phase stability (indicating that the source was not detected during this period) can be seen using CORPLOT.

Although the *a priori* gain calibration for each telescope is made in AIPS using the nominal gain and system temperatures, large residual, gain errors of up to 30% often persist. For this reason, observations of additional compact sources by the ground telescopes are scheduled (typically during gaps in HALCA tracking) and used to better constrain the gain values for each telescope. These calibrators have known structures from the VLBApl catalog (Fomalont et al. 2000b) and their flux densities monitored from observing programs at the University of Michigan² and at the Australia Telescope Compact Array (Tingay et al. 2003).

4.2. Self-Calibration and Imaging Iterations

Since most Survey experiments have limited (u, v) -coverage, imaging and/or model-fitting requires the introduction of constraints to the size and complexity of the radio emission in order to obtain accurate deconvolution and self-calibration. The first step is to make a relatively low resolution image without the HALCA data. These images provide the best

²<http://www.astro.lsa.umich.edu/obs/radiotel/umrao.html>

sensitivity to extended structure and help identify regions in the field where the most compact structure was likely to be located. The VLBApl catalog image, made from observations in 1996 (Fomalont et al. 2000b), as well as other pre-existing images of the sources (including ground observations at 15 GHz which had similar resolution of the VSOP Survey observations [Kellermann et al. 1998; Gurvits et al. 2004, in preparation]) are also useful in determining the constraints needed to image the VSOP Survey data. For about 5% of the VSOP Survey observations, it is clear that the visibility amplitude on the shortest projected baselines is much lower than that known from pre-existing VLBI observations, even considering possible variability of sources. This indicates that a problem has occurred at one or more antennas during the observation or during the tape copying process (if it was required) or during correlation. If the problem can not be rectified the observations are considered corrupted, and placed back into the VSOP Survey observing schedule for another observation. In cases such as these the data are processed, often as a ground-only observation, as they may still provide useful information.

The next imaging step includes all of the data to obtain an approximate image. For most sources, the (u, v) -coverage is sufficient to use CLEAN, followed by a phase-only self-calibration to improve the phase calibration. Several phase self-calibration iterations are generally made for each source. For sources with extremely poor (u, v) -coverage, model-fitting the data with one or two Gaussian-shaped components is used instead of the CLEAN deconvolution. In some cases a hybrid approach, using CLEAN components for the extended emission and models for the small-diameter components, is used. The use of various data weightings to emphasize or de-emphasize the longer VSOP baselines depends upon the strength and size of the source and the number of visibilities on ground-only baselines compared to ground-space baselines. To obtain images that best reveal the ~ 0.1 mas scale a weighting scheme is used for which the space-ground baselines contribute about 50% of the effective data. As an illustration of the importance of increasing the data weights on space baselines, we present the results of fitting a simple model to the VSOP Survey observations of 3C345 on 1998 July 28 (Figure 2). The MODELFIT procedure in Difmap applies a weight of $1/\sigma^2$ to each visibility point. When the weights are calculated in this way the sensitive ground-only visibilities dominate the fit and the ground-space baselines have little influence. However, if the HALCA data are upweighted, in this case by a factor of 25 so that ground-space and ground-only visibilities have roughly equal weighting, the fit improves significantly.

For most Survey experiments, amplitude self-calibration is not used due to lack of closure constraints and/or limited sensitivity of the space-baselines. In the cases where the data from four or more telescopes are sufficiently strong, amplitude self-calibration using GSCALE provides a scale factor for each telescope over the entire observation. In some cases, amplitude

self-calibration over a time-scale of one hour is possible.

4.3. Image Representation

A satisfactory image is generally obtained after three or four phase self-calibration loops and perhaps one amplitude calibration. Such a quick convergence is due to the limitations on the achievable image fidelity characterised by a sparse (u, v) coverage, and a lack of short spacings in particular. The latter typically contain most of the information on complex, extended structures. For most sources two representations of the source structure are available: the CLEAN image, and a model-fit image. For small-diameter components with poor (u, v) -coverage, the model representation is more reliable than the CLEANed image. In some cases, the CLEAN components more accurately reproduce the extended emission, while the Gaussian model component describes the small-diameter components more accurately. Both representations of the source structure should be in relatively good agreement, and satisfactorily fit the observed (u, v) -data.

The model representation of the source structure isolates important parameters of the components which are necessary to determine angular sizes and brightness temperatures. Even for images in which the CLEAN algorithm was used to determine the source structure, the models are chosen carefully, starting simple and moving to more complicated structures. The goal is to fit the observed visibilities within the uncertainties using the smallest number of model parameters, and to duplicate the structure found by cleaning. The following guidelines are used in choosing model components:

1. The number of components is kept to a minimum.
2. Simple components are preferred to complex ones, *i.e.* a point model is better than a circular Gaussian model which is better than an elliptical Gaussian component.
3. If an elliptical component becomes linear during model fitting it was generally an indication that the sampling of the (u, v) -plane was poorly constrained in the direction perpendicular to the component's major axis. In these cases, a circular Gaussian component is favored.
4. In general, additional or more complex components are used only if the data or the image require it.

The calibrated data, models and cleaned image are then saved in the NRAO AIPS UVFITS format using Difmap's SAVE command. These data can be read back into Difmap

for further processing, imaging and modeling, and are available through the VSOP Survey Data Base Web site.

5. VSOP Survey Data Base

Once a data analyst has completed the reduction of an experiment, the calibrated data, reduction notes and supporting files (from both AIPS and Difmap) are uploaded to a computer at ISAS. Information from the uploaded files is entered into a database and published on the VSOP Survey web page (<http://www.vsop.isas.jaxa.jp/survey>). Displays of the final calibrated visibilities, images (CLEAN and model-fit), and the model fit parameters are available. Documentation of the data processing, from the initial calibration, to the fringe-fitting, to the imaging and modeling, are given for each experiment. The calibrated data are available from the web site and the original post-correlation data can be obtained upon request, but this dataset is much larger (of the order of 100 Mb compared to ~ 100 kb).

6. Conclusion

This paper, the second in the VSOP 5 GHz AGN Survey series, has described the data processing used to construct the images and determine models from the VSOP Survey Program. Because of the uniqueness of the Space VLBI Survey data, we have described many of the procedures in some detail since they are different from normal VLBI reduction practices. Enhancement of the data procedures and the development of new algorithms (especially for detecting weak sources) are needed for further space VLBI missions.

The National Radio Astronomy Observatory is a facility of the National Science Foundation operated under cooperative agreement by Associated Universities, Inc. This research has made use of data from the University of Michigan Radio Astronomy Observatory, which is supported by funds from the University of Michigan. J.E.J.L., G.A.M., and R.G.D. each acknowledge the support of Japan Society for the Promotion of Science fellowships. W.K.S. and A.R.T. wish to acknowledge support from the Canadian Space Agency.

REFERENCES

- Carlson, B. R., Dewdney, P. E., Burgess, T. A., Casorso, R. V., Petrachenko, W. T., & Cannon, W. H. 1999, PASP, 111, 1025

- Cotton, W. D. 1995, in ASP Conf. Ser. 82, Very Long Baseline Interferometry and the VLBA, eds. J. A. Zensus, P. J. Diamond and P. J. Napier (San Francisco: ASP), 189
- Edwards, P. G., Hirabayashi, H., Fomalont, E. B., Gurvits, L. I., Horiuchi, S., Lovell, J. E. J., Moellenbrock, G. A., & Scott, W. K. 2002, 8th Asian-Pacific Regional Meeting, Volume II, 375
- Fomalont, E., et al. 2000a, in Proceedings of the VSOP Symposium, January 2000a, Astrophysical Phenomena Revealed by Space VLBI, eds. H. Hirabayashi, P. G. Edwards, & D. W. Murphy (Sagamihara: The Institute of Space and Astronautical Science), 167
- Fomalont, E. B., Frey, S., Paragi, Z., Gurvits, L. I., Scott, W. K., Taylor, A. R., Edwards, P. G., & Hirabayashi, H. 2000b, ApJS, 131, 95
- Greisen, E. W. 1988, in Acquisition, Processing and Archiving of Astronomical Images, eds. G. Longo & G. Sedmak (Napoli: Osservatorio Astronomico di Capodimonte), 125
- Horiuchi, S., et al., 2004, ApJ, submitted.
- Hirabayashi, H., et al. 1998, Science, 281, 1825
- Hirabayashi, H., et al. 2000a, PASJ, 52, 6, 955
- Hirabayashi, H., et al. 2000b, PASJ, 52, 6, 997
- Kellermann, K. I., Vermeulen, R. C., Zensus, J. A., & Cohen, M. H. 1998, AJ, 115, 1295
- Kobayashi, H., et al. 2000, PASJ, 52, 6, 967
- Lister, M. L., Tingay, S. J., Murphy, D. W., Piner, B. G., Jones, D. L., & Preston, R. A. 2001, ApJ, 554, 948
- Napier, P. J., Bagri, D. S., Clark, B. G., Rogers, A. E. E., Romney, J. D., Thompson, A. R., & Walker, R. C. 1994, IEEE Proc. 82, 658
- Scott, W. K., et al., 2004, ApJS, accepted.
- Shepherd, M. C. 1997, in ASP Conf. Ser. 125, Astronomical Data Analysis Software and Systems VI, eds. G. Hunt, & H.E. Payne (San Francisco: ASP), 77
- Shibata, K. M., Kamenno, S., Inoue, M., & Kobayashi, M. 1998, in ASP Conf. Ser. 144, Radio Emission from Galactic and Extragalactic Compact Radio Sources, eds. J. A. Zensus, G. B. Taylor, & J. M. Wrobel (San Francisco: ASP), 397

Tingay, S. J., Jauncey, D. L., King, E. A., Tzioumis, A. K., Lovell, J. E. J., & Edwards, P. G. 2003, PASJ, 55, 351

Whitney, A. R. 1999, New Astron. Rev., 43, 527

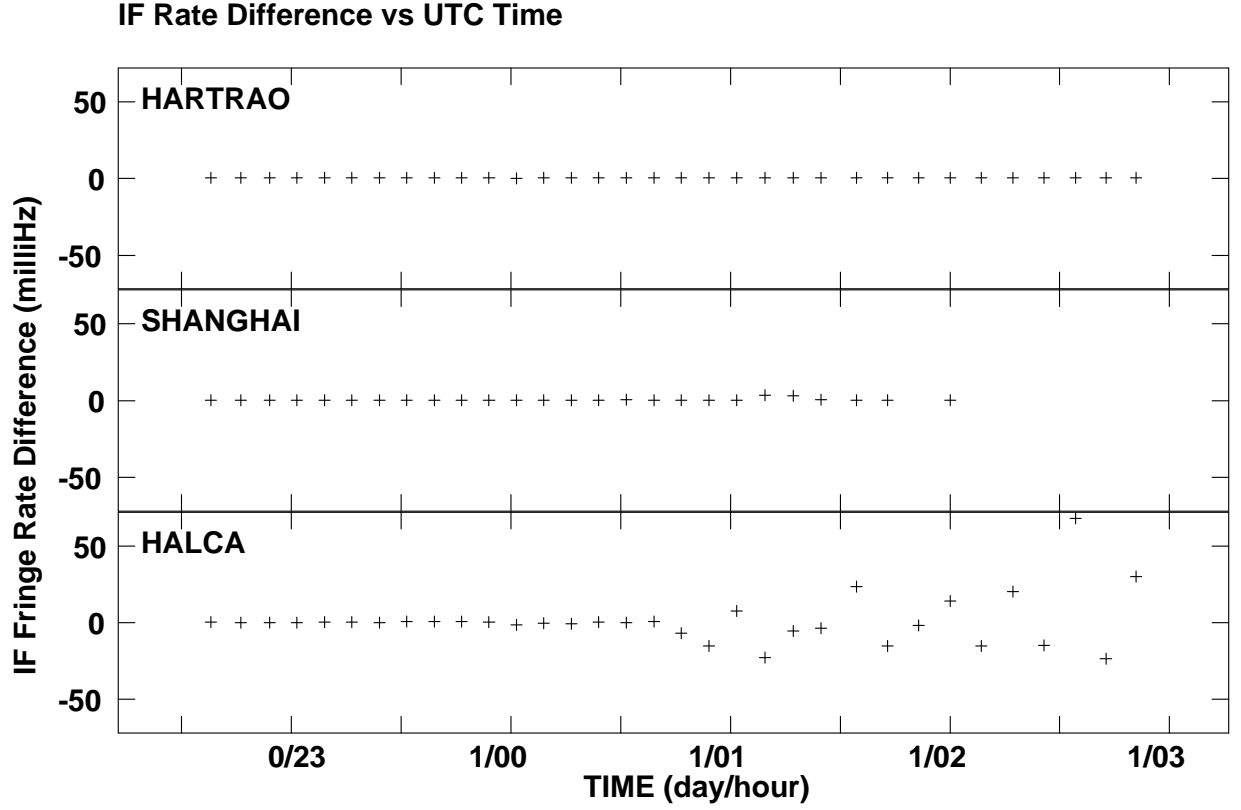


Fig. 1.— An example of the difference in fringe rate solutions between the two bands for a typical Survey experiment. Fringes to HALCA are detected until nearly 1/01 at which time the differences become randomly distributed on a scale exceeding the fringe rate resolution (~ 3 mHz FWHM). In this case the fringe rate search window was restricted which is why the rate differences are constrained after fringes are lost.

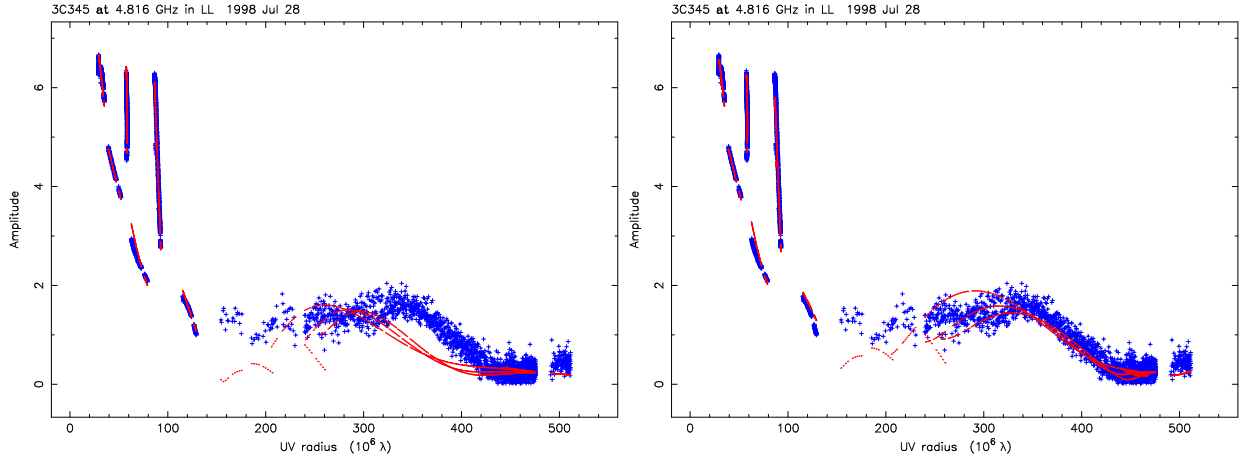


Fig. 2.— Model fits to the visibility data from a VSOP Survey observation of 3C345. Visibility amplitudes (+ symbols) and model visibilities (solid points) are plotted as a function of (u, v) radius. **Left:** the result of a fit using the standard $1/\sigma^2$ weighting and **right:** a model fit with the weight on HALCA data increased by a factor of 25.